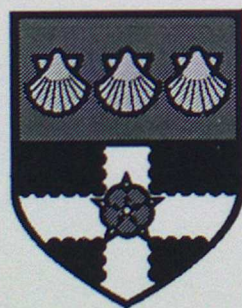# JCMM

Met Office

Comparison of ECMWF Winter-Season Cloud
Fraction with Radar Derived Values

Robin J. Hogan, Christian Jakob,
Anthony J. Illingworth

January 2001

INTERNAL REPORT No. 124

NWP Scientific Paper No. 338

Joint Centre for Mesoscale Meteorology

Comparison of ECMWF Winter-Season Cloud Fraction with Radar Derived Values

ROBIN J. HOGAN,* CHRISTIAN JAKOB[†] AND ANTHONY J. ILLINGWORTH

Department of Meteorology, University of Reading, United Kingdom
[†]*European Centre for Medium-Range Weather Forecasts, Reading, United Kingdom*

ABSTRACT

Of great importance for the simulation of climate using General Circulation Models is their ability to accurately represent the vertical distribution of fractional cloud amount. In this report, a technique to derive cloud fraction as a function of height using ground-based radar and lidar is described. The relatively unattenuated radar detects clouds and precipitation throughout the whole depth of the troposphere, while the lidar is able to accurately locate cloud base in the presence of rain or drizzle. From a direct comparison of three months of cloud fraction observed at Chilbolton, England with the values held at the nearest gridbox of the ECMWF model we find that, on average, the model tends to under-predict cloud fraction below 7 km and considerably over-predict it above. The difference below 7 km can in large part be explained by the fact that the model treats snow and ice cloud separately, with snow not contributing to cloud fraction. Modifying the model cloud fraction to include the contribution from snow (already present in the form of fluxes between levels) results in much better agreement in mean cloud fraction, frequency of occurrence and amount when present between 1 km and 7 km. This, together with the fact that both the lidar and the radar echos tend to be stronger in the regions of ice clouds that the model regards as snow, indicates that snow should not be treated as radiatively inert by the model radiation scheme. Above 7 km the difference between the model and the observations is partly due to some of the high clouds in the model being associated with very low values of ice water content that one would not expect the radar to detect. However, removal of these from the model still leaves an apparent overestimate of cloud fraction by up to a factor of two. We also find a tendency in the lowest kilometer for the model to simulate cloud features up to three hours before they are observed. Overall this study demonstrates the considerable potential of active instruments for validating the representation of clouds in models.

1. Introduction

It is well known that clouds play a fundamental role in the earth's radiation budget and that the representation of clouds in General Circulation Models (GCMs) is one of the major factors limiting the accuracy of future climate prediction (Arking 1991; IPCC 1995). The limited spatial resolution available to current GCMs means that in addition to the usual cloud variables of liquid and ice water content, it is necessary for them to include some estimate of the fractional cloudiness in each gridbox. Most models diagnose cloud fraction every timestep from prognostic model variables such as humidity or total water content (Slingo 1987; Smith 1990), but in the current version of the European Center for Medium-Range Weather Forecasts (ECMWF) model, cloud fraction is itself formulated as a prognostic variable (Tiedtke 1993). Whether diagnostic or prognostic, the physical basis underlying the treatment of this parameter is somewhat uncertain, and consequently errors in model radiative fluxes are often blamed on poor model cloud fraction. GCM studies have shown that these errors can then feed through into precipitation and circulation patterns (Slingo and Slingo 1988; Randall et al. 1989).

A common way to test the representation of clouds in models is to compare upwelling top-of-atmosphere fluxes from the model with satellite measurements, using either the broadband Outgoing Longwave Radiation (e.g. Slingo 1987), or brightness temperature in specific satellite long-wave window channels (Morcrette 1991). This approach is useful to evaluate the overall radiative impact of the model clouds but is hampered by the fact that the radiative fluxes represent integrals over many parameters, such as cloud fraction, cloud water content, cloud top height, atmospheric conditions above the cloud and the micro-physical cloud properties. A further complication is that low clouds, which have a brightness temperature close to that of the surface, are not easily detected.

A large number of cloud products are now generated routinely by the International Satellite Cloud Climatology Project (ISCCP) from both the visible and infrared channels of the various meteorological satellites. Jakob (1999) compared monthly-mean total cloud cover from the ECMWF Reanalysis (in which no observational data were used to directly alter clouds) against the ISCCP values and identified a number of biases, including an underestimate of extratropical cloud cover over the ocean by 10% to 15% and an overestimate of trade wind cumulus by the same amount. Similarly, Karlsson (1996) found from a two-month comparison with AVHRR data over the Scandinavian region that the ECMWF model underestimated total cloud cover by 13%. He also found that the fraction of the total cloud cover attributable to 'high' clouds was greater in the model by up to a factor of two.

The principal limitations of such passive measurements are the lack of vertical resolution and the poor penetration when multiple cloud layers are present. Furthermore, the total cloud cover calculated from model fields depends not only on the values of cloud fraction at each model level, but also on the overlap assumption; the difference in predicted total cloud cover between assuming 'maximum' and 'random' overlap is typically around 10%

Corresponding author address: Department of Meteorology, Earley Gate, PO Box 243, Reading RG6 6BB, United Kingdom. E-mail: R.J.Hogan@reading.ac.uk.

(e.g. Morcrette and Jakob 2000), of comparable magnitude to the differences found by Karlsson (1996) and Jakob (1999). There is clearly a need for high vertical resolution observations by active instruments to overcome these problems by measuring cloud fraction at each model level. Mace et al. (1998) compared hydrometeor occurrence from three months of 35-GHz radar data with the same information held in the ECMWF model, and found the model to have good overall skill at predicting the mean vertical distribution of clouds, despite some problems in the timing of the onset and dissipation of deep cloud events. The distinct advantages of active instruments were demonstrated, but in their study the radar was used only to determine whether or not any cloud or precipitation had occurred in each 30 minute period; cloud fraction was not calculated.

In this study, three months of radar and lidar observations at Chilbolton, England during the winter of 1998/1999 are used to derive cloud fraction for comparison with the ECMWF model. The same dataset was used by Hogan and Illingworth (2000) to characterize the degree of cloud overlap for use in GCMs. Throughout most of the depth of the atmosphere one of two vertically-pointing cloud radars is used, but up to the freezing level we also use the cloud base reported by a lidar ceilometer. The details of the model and the observational data used in the study are outlined in section 2, and in section 3 the technique is described. In section 4 the observed cloud fraction climatology is compared directly with the values held in the model, and in section 5 the comparison is refined to account for important differences in the treatment of both snow and very thin cirrus, allowing a more detailed analysis be performed in section 6.

2. Description of the data

a. Instruments at Chilbolton

The primary observational data used in this study were taken by the two vertically-pointing cloud radars located at Chilbolton in Southern England, between 24 October 1998 and 23 January 1999. The 35-GHz 'Rabelais' radar was operational from the start of the experiment until 20 November, and the 94-GHz 'Galileo' was operational from 5 November until the end of January. Together they collected a near-continuous dataset of radar reflectivity factor (Z), which in the Rayleigh-scattering regime we define as

$$Z = 10 \log_{10} \left(\sum_{vol} \frac{|K|^2}{0.93} D^6 \right) \quad \text{dBZ},$$

where D is the particle diameter in millimeters, and $|K|^2$ is the 'dielectric parameter'. The factor of 0.93 is present to make Z relative to liquid water at centimeter wavelengths.

For extra sensitivity the raw pulses were averaged over 2 minutes and 2 range-gates (where the range-gate spacing was 75 m at 35 GHz and 60 m at 94 GHz). This re-

sulted in minimum-detectable reflectivity factors at 1 km of around −50.5 dBZ at 35 GHz and −52.5 dBZ at 94 GHz. Hence in the period when both radars were operational, the 94-GHz radar was invariably used for the comparison with the model because of its nominally higher sensitivity, and in the end less than a fifth of the three-month comparison was performed with 35-GHz data. It is our experience that radar calibration using an RF link budget can be very error prone (especially for a bistatic system such as the 94-GHz Galileo), so our approach was to compare Z values at 35 and 94 GHz with those at 3 GHz in drizzle, which Rayleigh scatters at all three frequencies. The 3-GHz weather radar at Chilbolton was absolutely calibrated to within 0.5 dB using the redundancy of the polarization parameters in heavy rain (Goddard et al. 1994), so we believe that the calibration of the two cloud radars should be accurate to around 1.5 dB.

Below the melting level we made use of the continuous observations of the 905 nm Vaisala CT75K lidar ceilometer at Chilbolton, which records 30-s averaged profiles of lidar backscatter coefficient (β) with a vertical resolution of 30 m. The output from this commercial instrument also includes cloud base height as diagnosed from the β profile. In practice liquid water clouds always give strong echos and the sharp gradient at cloud base can easily be picked out by the lidar.

Measurements were also taken by a drop-counting raingauge, and were used to identify when attenuation by rain could potentially have been a problem for the 94-GHz radar.

b. ECMWF model fields

The model data used in this study were extracted from daily operational ECMWF forecasts. Each day the model's 12 to 35 hour forecast (00 UTC to 23 UTC) for the model gridbox closest to Chilbolton (centered 25 km to the north-west of the site) was used, and long time series were created by concatenating consecutive model forecasts. The ECMWF spectral model uses T_L319 truncation, corresponding to a horizontal resolution of around 60 km. At the time of the comparison it had 31 vertical levels, with a spacing of around 400 m at 1.5 km and around 800 m at 10 km. The timestep of the model was 20 minutes, although only the hourly fields were recorded. In April 1995 the model was upgraded from the diagnostic formulation for cloud fraction of Slingo (1987) to a prognostic scheme which includes source terms from condensation, convection and boundary-layer turbulence and a sink term corresponding to evaporation (Tiedtke 1993). The agreement with conventional human observations of total cloud cover improved immediately. The main purpose of this study is to test the performance of the new scheme at each model level.

2

3. Method

The principle of the technique is straightforward; daily time-height sections of radar reflectivity are divided into boxes of 1 hour duration centered on the model height levels, and cloud fraction is taken to be the fraction of radar pixels in each box that register the presence of cloud. For example, at a height of 5 km where the level spacing is 600 m, the 35-GHz radar with its 2 min/150 m pixel size records 120 pixels in each box, allowing cloud fraction to be discretized to better than 0.01. Radar is relatively unattenuated by cloud, enabling it to detect multiple layers through the whole depth of the atmosphere. However, it has some limitations in the lowest 2 km which can be overcome only with the extra information provided by the lidar.

Firstly, radar returns below around 400 m cannot be used because of leakage by the transmit pulse into the receiver and the presence of ground clutter. Consequently the radar cannot retrieve cloud fraction in the lowest two levels of the model. The lidar on the other hand is able to make measurements right down to the surface.

The second problem is that, because Z is proportional to the sixth power of particle diameter, the radar is unable to pick out the base of liquid water clouds in the presence of rain or drizzle as the signal is dominated by the contribution from these much larger drops. Lidar backscatter coefficient on the other hand is approximately proportional to the second power of diameter, so the base of liquid water clouds can always be identified as a sharp and substantial increase in β embedded within the weaker signal from the precipitation. It is found that even stratocumulus clouds often have sufficient drizzle falling out of them that cloud base height according to the radar alone is too low by several hundred meters. Invariably the signal from the lidar is rapidly extinguished in liquid water clouds and the radar must be used at higher levels.

A further problem often encountered in the interpretation of cloud radar data in the boundary layer is contamination of the meteorological signal by insects. At the latitude of Chilbolton during winter insects are simply never seen, but in principle a lidar could easily distinguish them from clouds because, as with raindrops, the typical value of β from these very large but low-concentration targets is very small.

To illustrate the complementary nature of the two instruments, Fig. 1 depicts 9 hours of observations in light precipitation associated with a warm front, overlayed by the model grid. The radar detects the full vertical extent of the cloud and precipitation, while the lidar records a very strong signal from the cloud base (which is not detected by the radar), above which it is rapidly extinguished. It also detects boundary-layer aerosols, although they give a much weaker echo and are never mistaken for cloud. Cloud base measured by the lidar is shown superimposed on the radar image, and is used to refine the cloud fraction diagnosed by the radar alone; in this case the cloud
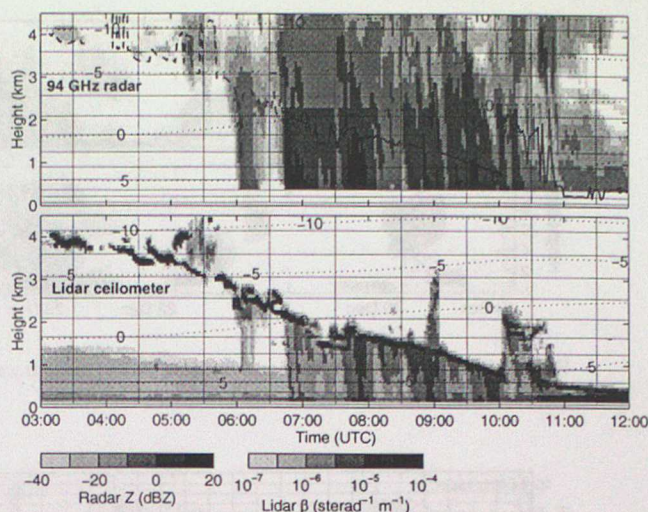

FIG. 1: Radar and lidar observations of light precipitation on 27 November 1998. Superimposed on the radar image is the position of cloud base according to the lidar, although above the melting layer it is not used in the retrieval of cloud fraction and is shown as a dashed line. The dotted contours depict the temperature in °C according to the model.

fraction in each gridbox entirely below cloud base is set to zero, and for those that straddle cloud base the cloud fraction can be calculated accordingly. However, the lidar is not used above the melting level (as diagnosed from the model temperature field), where we leave the original radar cloud fraction unaltered. The logic behind this is that there is no physically appropriate distinction between ice cloud and ice precipitation that can be exploited in the same way as that between liquid cloud and rain. In ice the radar and lidar returns tend to be rather similar in appearance, with typically very good agreement in the height of the lowest echo and no sharp gradient in the lidar β profile above to mark the transition from precipitation to cloud. In any case, the lidar usually cannot even penetrate as far as the melting level because of the common occurrence of strongly-attenuating stratocumulus. The issue of cloud/precipitation discrimination is discussed further in section 5a. When the lidar does detect a sharp gradient and a high value of β above the melting level it generally corresponds to a layer of supercooled liquid water; in Fig. 1 the strong echo of the liquid cloud base extends up through the 0°C isotherm to a height of 4 km where the temperature was -10°C. It would be difficult to explain the complete extinction of the lidar signal in only a few hundred meters as being due purely to ice crystals. Supercooled clouds such as this are fairly common at the leading edge of warm fronts.

We also use the lidar cloud base to compensate for the fact that some liquid water clouds are too low or too tenuous to be detected at all by the radar. If the lidar detects any cloud warmer than 0°C that is not seen by the radar, then cloud fraction is increased assuming that the cloud is no more than one model level deep. In practice it is rare for a low cloud to be completely undetected by the radar,
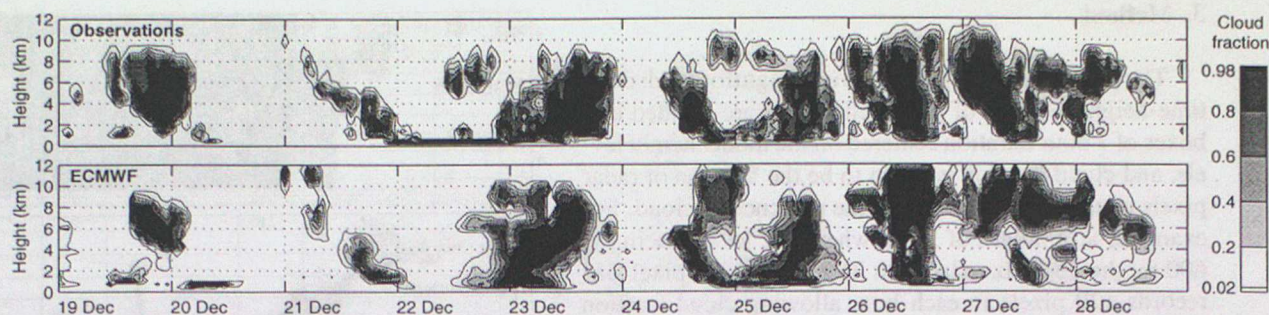
3

FIG. 3: Comparison of observed and ECMWF model cloud fraction at Chilbolton for a ten-day period in 1998. Only the 94-GHz radar was used during this time.
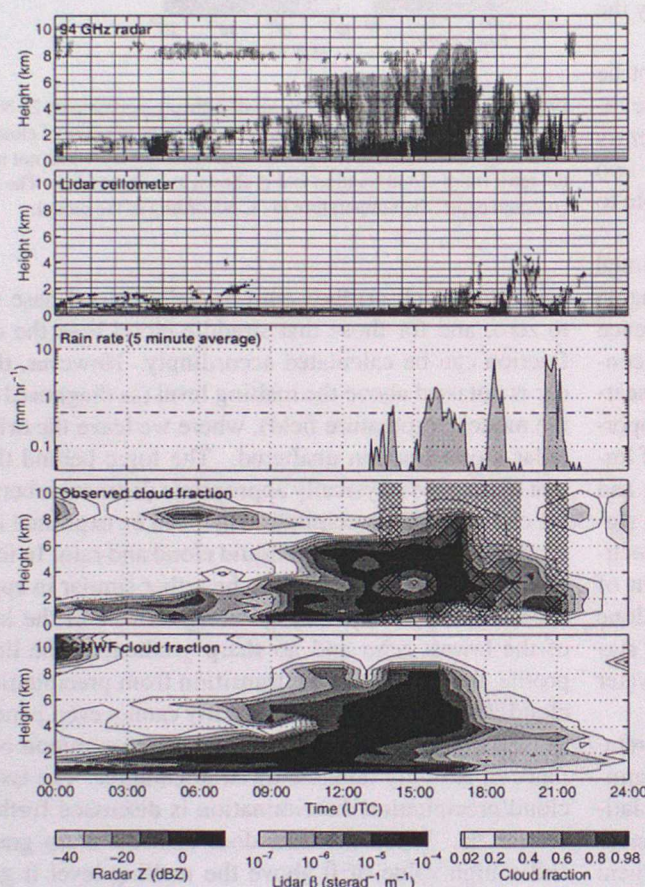

FIG. 2: An example of the retrieval of cloud fraction from radar and lidar data on 25 December 1998. Overlayed on the raw observations in the top two panels are the model grid boxes, and rain rate is shown in the third panel. The fourth panel depicts the cloud fraction retrieved from these observations, and the fifth shows the corresponding values held in the ECMWF model. The crosses on the observed cloud fraction field show periods when comparison with the model was not performed because the rain rate at the surface exceeded 0.5 mm hr^{-1} some time during the hour.

and it is usually only fog that is too low for the radar to detect.

Figure 2 demonstrates the retrieval of cloud fraction from a whole day of data. The top two panels show the raw radar and lidar echos, and the third panel shows rain rate. Because rain can occasionally strongly attenuate the 94-GHz signal, we do not use derived cloud fraction in the comparison when the rain rate at the ground exceeds 0.5 mm hr^{-1} (shown by the dot-dashed line) at any time during the hour-long accumulation period. At 94 GHz, a rain rate of 0.5 mm hr^{-1} corresponds to a two-way attenuation of around 1 dB km^{-1} (Lhermitte 1987). Indeed, the sharp decrease in observed high cloud in the radar image at around 18 UTC is probably due to attenuation by rain. However, less than 10% of the data were excluded in this way, and consequently the effect on the results was quite small. The fourth panel show the cloud fraction derived from the observations, and the simultaneous model values are shown in the last panel. The 0°C isotherm was at around 2.3 km on this day.

For the comparison with the model to be valid we are essentially assuming that in 1 hour the clouds sampled over a single point will be representative of the clouds in an entire 60 km gridbox. A windspeed of 17 m s^{-1} is sufficient for clouds at both sides of the gridbox to be sampled within the accumulation period, and this is only a little lower than the actual mean windspeed over the site, but of course it is still only a two-dimensional slice through a three-dimensional volume. In an attempt to match the timestep in the model an accumulation period of 20 minutes was also tried, but the resulting cloud fraction was found to be much noisier than the corresponding model field, probably because the sample was not sufficiently representative of the whole gridbox.

4. Direct comparison of observed and modeled cloud fraction

Cloud fraction has been calculated from the radar and lidar observations between 24 October 1998 and 23 January 1999 at Chilbolton, and Fig. 3 shows observed and modeled cloud fraction for a ten-day period in December 1998. The larger scale features appear to match up reasonably well, although there is certainly room for improvement.

Figure 4 shows mean cloud fraction as a function of height from both the model and the observations for the entire three-month period. We see a clear tendency for
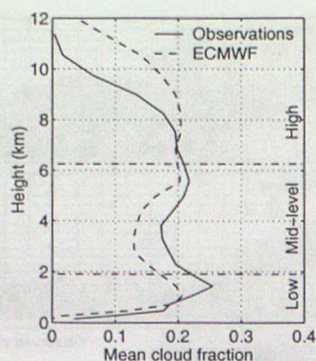
FIG. 4: Three-month mean cloud fraction as a function of height over Chilbolton according to both the observations and the model.
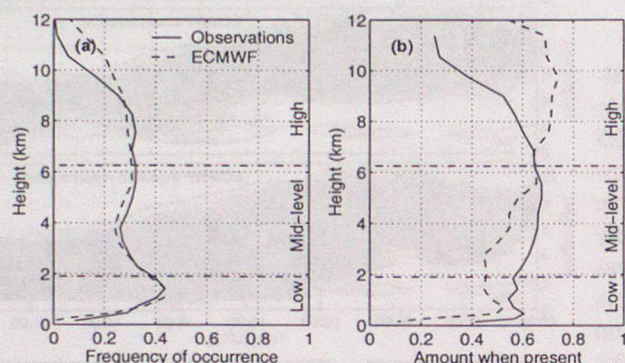

FIG. 5: Cloud fraction climatology split into (a) the frequency that the gridbox-mean cloud fraction was greater than 0.05, and (b) the mean cloud amount when greater than 0.05.

the model to underestimate cloud fraction below 7 km and overestimate it above. Figure 5 shows this information split up into 'frequency of occurrence' (similar to the parameter compared in the study by Mace et al. 1998) and 'amount when present', where cloud is deemed to be 'present' when the cloud fraction is greater than 0.05. The results are found to be fairly insensitive to the exact value of this threshold. Up to 9 km the frequency of occurrence agrees remarkably well, so it would seem that the differences in mean cloud fraction found in Fig. 4 are due almost entirely to systematic errors in simulating the amount of cloud when present. Above 9 km the model appears to overestimate frequency of occurrence.

5. Problems with the direct comparison

Direct comparison of the modeled and observed cloud fraction climatologies appears to have revealed systematic differences between the two, with the model tending to underestimate the amount when present at low and mid-levels, and overestimate it at high levels (Fig. 5b). In this section we explore the extent to which these discrepancies can be explained by differences in what does and what does not contribute to cloud fraction in the model and the observations, with the aim of providing a more robust diagnosis of any shortcomings of the model.
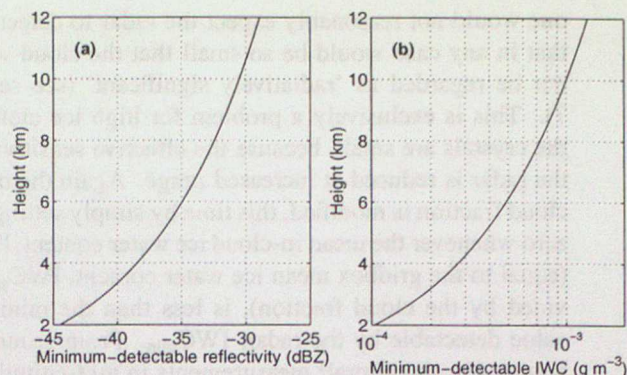

FIG. 6: Estimate of the minimum-detectable (a) reflectivity and (b) ice water content, as a function of height for both radars. This assumes a two-way attenuation of 2 dB of the 94-GHz signal through the boundary layer, resulting in a minimum-detectable reflectivity of −30.5 dBZ at 10 km, the same as the unattenuated 35-GHz value.

a. Snow/ice-cloud discrimination

As was outlined in section 3, there is a difficulty in making a fair comparison at mid-levels because, in contrast to the model, the observations cannot meaningfully distinguish precipitating snowflakes from nonprecipitating ice crystals. The interpretation of snow as cloud-free by the model probably explains why it generated around 25% less cloud between 1 km and 7 km than was observed.

Rather than make some artificial distinction between ice cloud and snow in the observations (such as from the absolute value of Z or the Doppler velocity), our approach is to modify the model cloud fraction to include the contribution from snow. This is done in a fairly simple manner; the gridboxes in each profile are examined sequentially from the top to the bottom, and whenever the snow flux from one level to the next exceeds some critical value *and* the cloud fraction in the lower of the two levels is less than that in the level immediately above, then the cloud fraction at the lower level is increased to equal that of the upper level. The critical snow flux should ideally represent the minimum value detectable by the radar, but unfortunately there is very little in the literature on the measurement of snowfall rates with millimeter-wave radars, for which large snowflakes scatter well outside the Rayleigh regime. Moreover, the model snow flux in any given profile rarely falls exactly to zero anywhere between the highest cirrus cloud and the melting layer, so if no critical value is set then this procedure would result in a huge increase in mid-level cloud fraction. For the remainder of this report we consider two melted-equivalent critical snowfall rates, 0.05 mm hr^{-1} (hereafter ECMWF1) and 0.1 mm hr^{-1} (hereafter ECMWF2).

b. Tenuous cirrus

The other problem with the comparison is that some of the high values of cloud fraction in the model may be accompanied by very small values of ice water content that

one would not reasonably expect the radar to detect, and that in any case would be so small that the cloud would not be regarded as 'radiatively significant' (see section 7). This is exclusively a problem for high ice clouds if the crystals are small, because the effective sensitivity of the radar is reduced at increased range. Again the model cloud fraction is modified, this time by simply setting it to zero whenever the mean in-cloud ice water content, IWC_{ic} (equal to the gridbox mean ice water content, IWC_{gb}, divided by the cloud fraction), is less than the minimum value detectable by the radar, IWC_{min}. From around 14 hours of in situ aircraft measurements in mid-latitude cirrus, Hogan and Illingworth (1999b) derived the following relationship between 94-GHz radar reflectivity (Z_{94}) and IWC:

$$\log_{10}(IWC) = 0.0706\,Z_{94} - 0.846,$$

where IWC has the units g m^{-3} and Z_{94} is in dBZ. As already stated, the 94-GHz radar has a minimum detectable reflectivity of -52.5 dBZ at 1 km, or equivalently -32.5 dBZ at 10 km. However, atmospheric gases (predominantly water-vapor in the boundary layer) attenuate the 94-GHz radar signal at cirrus altitudes by approximately 1 dB (two-way) during winter. Attenuation by liquid water clouds can also be significant, although this effect is much more variable. At 94 GHz the two-way attenuation by liquid water is around 9 dB km^{-1} per g m^{-3} at 5°C. For simplicity we assume a fixed attenuation of 2 dB, resulting in an effective sensitivity of -30.5 dBZ at 10 km, the same as that of the relatively unattenuated 35-GHz radar. Indeed, inspection of the data from when both radars operated together reveals little difference in the extent of cloud detected. Hence we use the same value of IWC_{min} for both radars. Figure 6 shows the minimum-detectable reflectivity as a function of height, with the corresponding IWC_{min} alongside.

c. Example of modified model cloud fraction

An example of the modification of model cloud fraction to both include the contribution from snow and exclude the contribution from undetectable cirrus is shown in Fig. 7. The unmodified model field contains virtually no cloud below 4 km until 12 UTC, whereas thick cloud is observed below 4 km from around 06 UTC onwards. Most of this difference is due to the model partitioning the ice into snow and cloud; when the model cloud fraction is modified to include the snow contribution, the agreement with observations is much better.

So the question to be answered is whether the radar is getting a disproportionately large signal from the snow in relation to its radiative importance (because of the sensitivity of Z to large particles), or whether the model is neglecting a radiatively important component from its calculation of cloud fraction. When we examine the lidar β field in Fig. 7, which in the absence of attenuation is a very good measure of radiative significance (because of its dependence on the second power of diameter and the
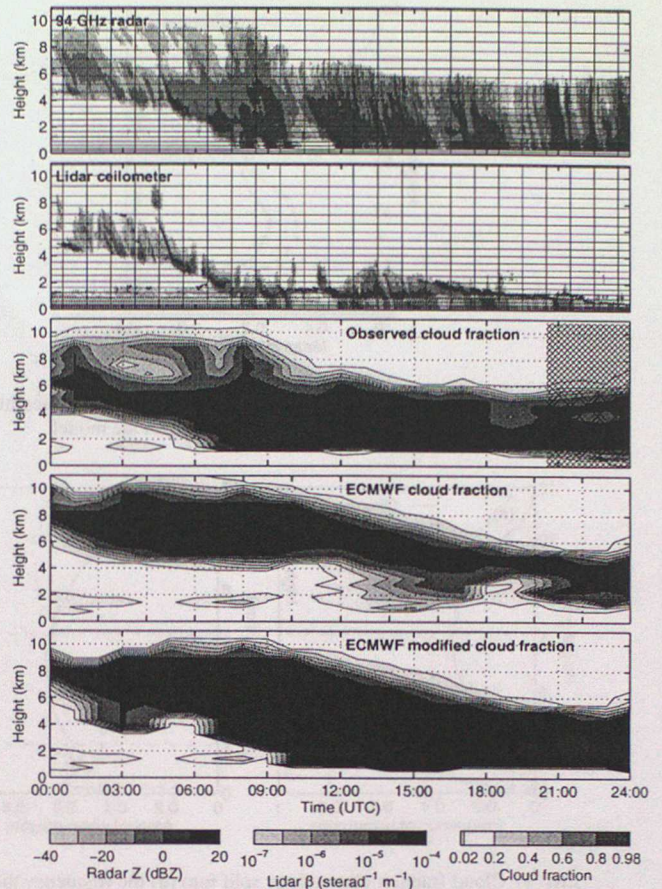

FIG. 7: Comparison from 13 November 1998, demonstrating the modification of model cloud fraction on a day with a substantial quantity of snow at mid-levels. The first two panels show the raw radar and lidar observations, and the third shows the cloud fraction derived from them. The fourth panel depicts the original model cloud fraction, and the last panel shows the same but after being modified to include the contribution from snow with a melted-equivalent snowfall rate in excess of 0.05 mm hr^{-1}, and to exclude very tenuous cirrus that would not be detectable by the radar (ECMWF1). As in Fig. 2, the crosses indicate where no comparison was performed because the rain rate exceeded 0.5 mm hr^{-1}.

vicinity of the lidar wavelength to the visible part of the spectrum), we find higher values in the 'snow' below 4 km than in the ice cloud above. This is also true of the radar reflectivity values. Moreover, it was found by Hogan and Illingworth (1999a) that the heights of the lowest radar and lidar echos in ice tend to agree very well—80% of the time to within 200 m and 96% of the time to within 400 m. Observations such as these challenge the philosophy of a having a separate snow variable that does not contribute to cloud fraction and is thus radiatively inert.

The removal of low-IWC cirrus has also had a visible effect on the model cloud fraction in Fig. 7, although the action of setting cloud fraction to zero has tended to sharpen the cloud top, in contrast to the observed cloud top which is characterized by many partially-filled gridboxes.
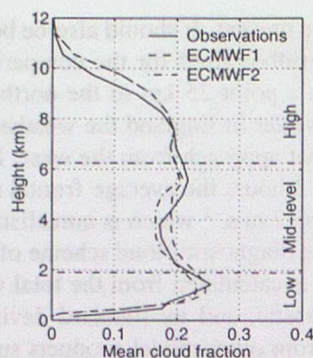
6

FIG. 8: Observed and modeled cloud fraction after modification of the model values to both exclude tenuous cirrus not seen by the radar and include the contribution from snow with a melted-equivalent snowfall rate greater than 0.05 mm hr^{-1} (ECMWF1) and 0.1 mm hr^{-1} (ECMWF2).

FIG. 10: Mean absolute difference in cloud fraction between the observations and ECMWF1 as a function of (a) height, and (b) time of day.
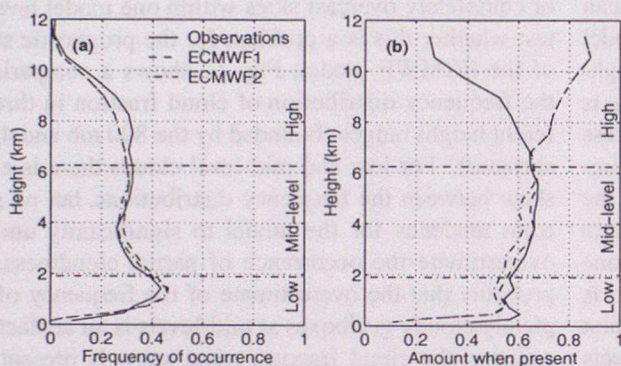

FIG. 9: The frequency of cloud occurrence and the mean amount when present for the observations and the two modified model fields that were used in Fig. 8.

6. Comparison using modified model cloud fraction

The comparisons of mean cloud fraction, frequency of occurrence and amount when present are repeated in Figs. 8 and 9 for the two modified model cloud fractions described in the last section, ECMWF1 and ECMWF2. The inclusion of snow makes a difference almost exclusively in the height range 1–6 km, whereas the exclusion of tenuous cirrus has a noticeable effect only above 7 km. Both have had the effect of bringing the model closer to the observations, and in Fig. 8 we see much better agreement in mean cloud fraction at all heights compared with Fig. 4, although there is still too much high cloud by up to a factor of two. The frequency of occurrence depicted in Fig. 9a still agrees very well below 9 km, because the addition of snow usually involves increasing cloud fraction where some cloud is already present. Above 9 km the agreement is much better than before; the exclusion of model IWC data below the radar detectability threshold has effectively more than halved the frequency of occurrence. The amount when present (Fig. 9b) now agrees significantly better at mid-levels, but above 7 km the previously large overestimate (Fig. 5b) now appears to be even worse. This is an artifact of crudely setting the cloud frac-
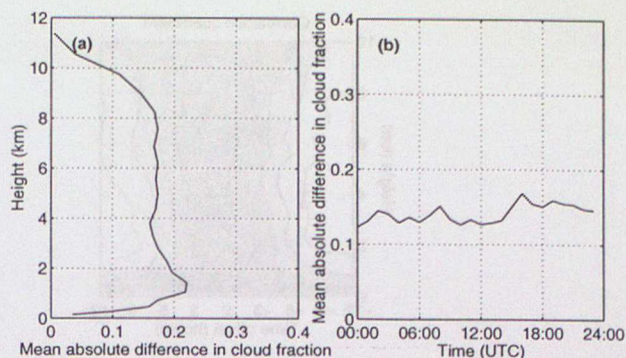
tion of a gridbox to zero when the mean in-cloud ice water content (IWC$_{ic}$) is deemed too tenuous to be detected by the radar, as there are more occasions in the dataset with low rather than high cloud fraction when IWC$_{ic}$ is below the radar detectability threshold. Had we assumed some kind of spatial variation of IWC within the cloudy part of each model gridbox then the removal of undetectable cloud would have involved a partial reduction of cloud fraction in a larger number of gridboxes, and the resulting amount when present would have had much more realistic values. However, such an assumption of spatial variation would have had no effect on mean cloud fraction, which depends only on the value of IWC$_{min}$, so the finding of an overestimate in high-level mean cloud fraction (Fig. 8) is still valid.

The addition of snow does not seem to have had an effect below 750 m where there is still an apparent underestimate of the amount when present; below 300 m the difference exceeds 0.3 (around a factor of 2.5). It is possible that the thickness of these low clouds is overestimated by the observations when it is assumed that, in the absence of any signal in the radar, they extend upwards from the lidar-measured cloud base to the top of the gridbox. One should remember that in the model radiation scheme it is assumed that clouds fill gridboxes vertically, whereas a cloud fraction of 0.5 in the observations could in principle correspond to a cloud *cover* of 100%, if the cloud was concentrated in the top or bottom half of the box. Thus it would seem certain that the model is underestimating the contribution to cloud cover from the clouds in the lowest 750 m, and probably underestimating cloud fraction as well.

Clearly modifying the model fields has resulted in a significantly better overall agreement with the observed climatology, but we still need to verify that clouds in the model occur at the right time. The ECMWF1 modified model cloud fraction (corresponding to a critical snow flux of 0.05 mm hr^{-1}) produces slightly better agreement than ECMWF2, so for the comparisons in the remainder of this section we use ECMWF1.

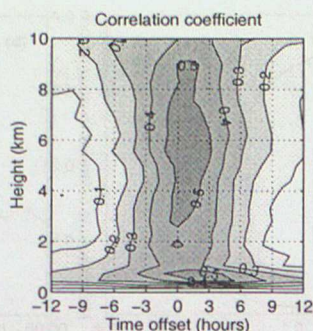First we determine how much, on average, the model

FIG. 11: The correlation coefficient between the observations and the model as a function of height and lag time, where a positive lag indicates a tendency for the model to simulate features before they were observed.

is in error at any given instant. Figure 10a shows the mean absolute difference in cloud fraction between the model and the observations as a function of height. Throughout most of the depth of the atmosphere the difference is around 0.17. In Fig. 8 we see that this is not much less than the typical mean cloud fractions of around 0.2, implying that the model is performing poorly. However, the requirement that the model should be accurate to within one hour and one model level is overly stringent, and one should bear in mind that the model radiation scheme is not run every timestep. It would perhaps be fairer to first average both fields onto a coarser grid that better reflects the spatial and temporal accuracy required.

Mean absolute difference is shown as a function of time of day in Fig. 10b, and we see that there is a slight tendency for the error to increase through the day. This is simply because the model fields were produced on a daily basis from forecasts initialized at 12 UTC the previous day, and the accuracy of the model naturally decreases with time. It also explains the abrupt changes sometimes seen in model cloud fraction at midnight, between the last hour of one daily forecast and the first hour of the next.

So if the model is performing poorly on a pixel-by-pixel comparison and yet the mean values are accurate, is it simply simulating clouds too early or too late? Figure 11 depicts the correlation between the two fields as a function of height and time offset. We see that throughout most of the depth of the atmosphere, as should be expected, the correlation coefficient is highest (at around 0.5) when there is no time lag between the two fields. However, in the lowest kilometer the maximum correlation occurs with a positive offset, indicating a surprising tendency for the model to simulate cloud features up to three hours before they were observed. This is somewhat difficult to explain. A possibility is that the diurnal cycle in the model is wrong and, for example, the transition from a stable nocturnal boundary layer to a well-mixed stratocumulus-topped daytime boundary layer occurs too rapidly after sunrise. However, it is interesting to note that when the lagged correlation is performed on separate 6-hour periods through the entire day, the same tendency

is always present. It should also be borne in mind that the model gridbox used for the comparison is actually centered on a point 25 km to the north-west of Chilbolton, and in winter in England the weather is characterized by fronts that approach from the west. However, to produce a lag of 3 hours the average frontal speed would have to be around 2 m s^{-1} which is unrealistically small.

In the diagnostic cloud scheme of Smith (1990), cloud fraction is calculated from the total water content, which is prognostic, and its standard deviation, which is estimated from other model products such as as Richardson Number. It is easy to imagine that if the model had a tendency to underestimate the standard deviation of total water content then, although the mean cloud fraction might be correct, the instantaneous values would too often take the extremes of 0 or 1 (corresponding to completely clear or completely overcast skies within one model level). To test whether this is a problem for the prognostic scheme of the ECMWF model, Fig. 12 shows a comparison of the frequency distribution of cloud fraction in three different height ranges (bounded by the 800 mb and 450 mb surfaces). For low and mid-level clouds there is a slight skew between the frequency distributions, but no significant tendency for the model to significantly under- or overestimate the occurrence of partial cloudiness. It is probable that the overestimate of the frequency of completely cloudy gridboxes at mid-levels is an artifact of increasing the cloud fraction when snow is present to be equal to the largest cloud fraction above. For high clouds there does seem to be a strong tendency for the model to predict partial cloudiness too infrequently, but this is not really meaningful because, as discussed above, the process of removing tenuous cirrus from the model so that the comparison of mean cloud fraction was fair involved the disproportionate removal of partial cloudiness events.

7. Discussion and conclusions

A technique for deriving cloud fraction from radar and lidar data has been developed and successfully implemented in a three-month comparison with the ECMWF model. The very-different scattering properties of radar and lidar were found to complement each other well, and in particular allowed cloud fraction to be accurately calculated even in the presence of drizzle and light rain.

Direct comparison between the model and the observations revealed that the model was excellent at simulating the frequency of cloud occurrence, but that it tended to underestimate the amount when present at mid-levels and overestimate it at high levels. The difference at mid-levels was found to be largely attributable to the exclusion of snow from the consideration of cloud fraction in the model, and it was also found that some cirrus clouds in the model were associated with ice water contents too low be detected by the radar. Adjustment of the model cloud fraction field to both include snow and exclude tenuous cirrus resulted in considerably better agreement with
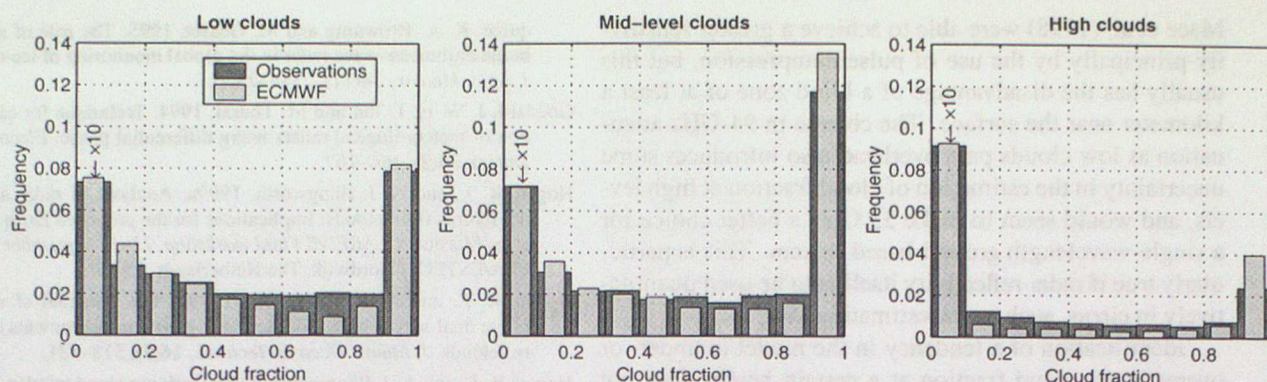
FIG. 12: Frequency distribution of observed and modeled cloud fraction in the three different height bands commonly used in ECMWF model parameterizations, bounded by the 800 mb and 450 mb surfaces. The model values have been modified as described for ECMWF1 in Fig. 8. Note that the frequencies corresponding to cloud fractions between 0 and 0.1 are shown at a tenth of their true magnitudes.

the observations. In particular it was found that:

- Below 750 m the model underestimated amount when present by up to 0.3.

- Between 750 m and 7 km excellent agreement was found between mean cloud fraction, frequency of occurrence and amount when present.

- Above 7 km the model was found to overestimate mean cloud fraction by up to a factor of two, even after the IWC threshold had been applied to remove 'undetectable' cirrus.

- The pixel-by-pixel correlation coefficient between the observed and modeled cloud fraction was around 0.5 at all heights.

- In the lowest 1 km the model tended to simulate cloud features up to 3 hours before they were observed.

However, the fact that two adjustments of the model field were necessary means that the results of the comparison affected by them should be considered more carefully.

Regarding the incorporation of snow into the model cloud fraction, we have shown that ice does exist in the form of snow in the model to make up for the underprediction of cloud fraction at mid-levels, and that use of a 'critical snow flux' of 0.05 mm hr^{-1} leads to very good agreement in both frequency of occurrence and amount when present. However, the radiation scheme still 'sees' the unmodified cloud fraction profile, despite the fact that the observations (most significantly those of the 905 nm lidar) clearly show snow to often be more optically thick than the ice cloud above it. Moreover, the observations do not show any sharp distinction between ice cloud and ice precipitation (Fig. 7) in the same way that they do between liquid water cloud and rain (Fig. 1), which suggests that it is more physically meaningful to treat ice cloud and snow together as a single variable (e.g. Wilson and Ballard 1999). The inclusion of snow in the radiation scheme

would probably not significantly affect Outgoing Longwave Radiation, but could be important for the radiative heating profile at mid-levels. The fact that we were able to achieve such good agreement at mid-levels by a simple modification of the model field based on snow flux suggests that the model could do the same. It should be noted that the value of critical snow flux that gave the best agreement in this study is not necessarily transferable between models; because the distinction between ice cloud and ice precipitation is somewhat arbitrary, the dividing line between the two would be expected to occur at a different point in other models.

In the case of tenuous cirrus, adjustment of the model fields was necessary to account for a deficiency of the observations rather than of the model, and although it reduced the amount of high cirrus it still resulted in an apparent overestimation of cloud fraction by up to a factor of two above 7 km. Despite the agreement with the study of Karlsson (1996), this result is unfortunately not as robust a finding as we would like because around a third of the total cloud volume above 8 km had to be removed from the model, and because there were inherent inaccuracies in our calculation of the minimum-detectable IWC. The clouds removed from the comparison typically had an IWC of less than 10^{-3} g m^{-3}, which for a 1 km thick cloud with an effective ice crystal radius of 10 μm corresponds to an infrared optical depth of only 0.08. This is around the 'radiative significance' threshold proposed by Brown et al. (1995) for mid-latitude cirrus. The optical depths in the ECMWF model would be even lower as the model radiation scheme uses an effective ice particle radius (and implied particle concentration via IWC) which varies with temperature from 40 μm at $-55°$C to 140 μm at $-20°$C (Ou and Liou 1995).

One could legitimately argue that the importance of cloud fraction for the radiation budget is much less in the case of very optically thin cloud, but only observations by a more sensitive radar could establish whether the low-IWC clouds that the model is simulating really exist.

9

Mace et al. (1998) were able to achieve a greater sensitivity principally by the use of pulse compression, but this usually has the disadvantage of a blind zone of at least a kilometer near the surface. The change in 94-GHz attenuation as low clouds pass overhead also introduces some uncertainty in the estimation of cloud fraction at high levels, and would seem to make 35 GHz a better choice for a single-wavelength ground-based system. This is particularly true if radar reflectivity itself is to be used quantitatively in cirrus, such as for estimating IWC.

Identification of a tendency in the model to under- or overestimate cloud fraction at a certain height does not necessarily indicate which part of the model needs modification. Even if the cloud scheme were perfect, any errors in the underlying dynamics would still feed through to cloud fraction. There is plenty of scope for further analysis of these data to address this issue, and one particular approach might be to composite the observations by synoptic type in order to expose tendencies for the model to consistently simulate certain features badly, such as the slope of fronts or the formation and dissipation of jet-stream cirrus and anticyclonic stratocumulus. This would then point towards which particular parameterization was in need of attention.

It should be noted that because the comparison was carried out during winter at a site in the mid-latitudes, convection was unimportant in generating clouds and the study is therefore essentially a validation of the stratiform part of the cloud parameterization. It would be very interesting to apply the technique during mid-latitude summer or in the tropics where convection is much more significant. The fact that the model has been shown to be reasonably good at simulating the presence of cloud opens the way for a more detailed comparison of model cloud parameters such as water content and particle size with the values derived by active ground-based instruments. The proposed spaceborne cloud radar and lidar (scheduled for launch in 2003 as part of the NASA Earth System Science Pathfinder Program) would be able to extend this over the whole globe. This study also highlights the possibility that such instruments could provide real-time information on clouds for assimilation into models.

REFERENCES

Arking, A., 1991: The radiative effects of clouds and their impact on climate. *Bull. Am. Meteor. Soc.*, **71**(6), 795–813.

Brown, P. R. A., A. J. Illingworth, A. J. Heymsfield, G. M. McFar-quhar, K. A. Browning and M. Gosset, 1995: The role of spaceborne millimeter-wave radar in the global monitoring of ice-cloud. *J. Appl. Meteor.*, **34**(11), 2346–2366.

Goddard, J. W. F., J. Tan and M. Thurai, 1994: Technique for calibration of meteorological radars using differential phase. *Electronics Letters*, **30**(2), 166–167.

Hogan, R. J., and A. J. Illingworth, 1999a: Analysis of radar and lidar returns from clouds: Implications for the proposed Earth Radiation Mission. *CLARE'98 Final workshop, 13–14 September 1999*, ESA/ESTEC, Noordwijk, The Netherlands, 75–80.

Hogan, R. J., and A. J. Illingworth, 1999b: The potential of spaceborne dual-wavelength radar to make global measurements of cirrus clouds. *J. Atmos. Oceanic Technol.*, **16**(5), 518–531.

Hogan, R. J., and A. J. Illingworth, 2000: Deriving cloud overlap statistics from radar. *Quart. J. Roy. Meteor. Soc.*, **126**(569A), 2903–2909.

Intergovernmental Panel on Climate Change (IPCC), 1995: *IPCC Second Assessment Report–Climate Change 1995*, UNEP/WMO.

Jakob, C., 1999: Cloud cover in the ECMWF reanalysis. *J. Climate*, **12**(4), 947–959.

Karlsson, K. G., 1996: Validation of modelled cloudiness using satellite-estimated cloud climatologies. *Tellus A*, **48**(5), 767–785.

Lhermitte, R. M., 1987: A 94 GHz Doppler radar for cloud observations. *J. Atmos. Oceanic Technol.*, **4**, 36–48.

Mace, G. G., C. Jakob and K. P. Moran, 1998: Validation of hydrometeor occurrence predicted by the ECMWF using millimeter wave radar data. *Geophys. Res. Let.*, **25**(10), 1645–1648.

Morcrette, J.-J., 1991: Evaluation of model-generated cloudiness: Satellite-observed and model-generated diurnal variability of brightness temperature. *Mon. Weath. Rev.*, **119**(5), 1205–1224.

Morcrette, J.-J., and C. Jakob, 2000: The response of the ECMWF model to changes in cloud overlap assumption. *Mon. Weath. Rev.*, **128**(6), 1707–1732.

Ou, S.-C., and K.-N. Liou, 1995: Ice microphysics and climate temperature feedback. *Atmos. Res.*, **35**, 127–138.

Randall, D. A., Harshvardhan, D. A. Dazlich and T. G. Corsetti, 1989: Interactions among radiation, convection and large-scale dynamics in a general-circulation model. *J. Atmos. Sci.*, **46**(13), 1943–1970.

Slingo, J. M., 1987: The development and verification of a cloud prediction scheme for the ECMWF model. *Quart. J. Roy. Meteor. Soc.*, **115**, 899–927.

Slingo, A., and J. M. Slingo, 1988: The response of a general circulation model to cloud long-wave radiative forcing: I. Introduction and initial experiments. *Quart. J. Roy. Meteor. Soc.*, **114**, 1027–1062.

Smith, R. N. B., 1990: A scheme for predicting layer clouds and their water content in a general circulation model. *Quart. J. Roy. Meteor. Soc.*, **116**, 435–460.

Tiedtke, M., 1993: Representation of clouds in large-scale models. *Mon. Weath. Rev.*, **121**, 3040–3061.

Wilson, D. R., and S. P. Ballard, 1999: A microphysically based precipitation scheme for the UK Meteorological Office Unified Model. *Quart. J. Roy. Meteor. Soc.*, **125**, 1607–1636.